04

Peculiarities of electrodispersion of metal microdroplets in laser torch plasma

© A.A. Bormatov, V.M. Kozhevin, D.A. Yavsin

Ioffe Institute, St. Petersburg, Russia
E-mail: antonbormat@mail.ru

Received August 5, 2024
Revised January 9, 2025
Accepted February 5, 2025

The paper considers the conditions for the development of electrocapillary instability on the surface of micron and submicron metal droplets in laser torch plasma. Using a numerical model of the Langmuir layer, it is shown that the condition for the development of electrocapillary instability on the droplet surface in plasma differs significantly from the Rayleigh criterion. A dispersion relation was obtained for waves on the surface of the melt under the influence of plasma.

Keywords: laser electrodispersion, electrocapillary instability, laser plasma, cascade division.

DOI: 10.61011/TPL.2025.05.61052.20084

Earlier experiments on nanosecond laser ablation of metals in vacuum have revealed a special ablation regime [1] with structures consisting of amorphous nanoparticles of the ablated metal, which are several nanometers in diameter and are characterized by an extremely narrow size dispersion, forming on a substrate located at a distance of several centimeters from the target surface. A method for synthesis of similar nanostructures from various metals (the laser electrodispersion method) has been developed based on this effect and has found application, e.g., in the production of catalysts with high catalytic activity and chemical stability [2].

The method of laser electrodispersion of metals relies on cascade fragmentation of submicron metal droplets ejected from the target surface into laser torch plasma, where they are charged by the flux of plasma electrons (Fig. 1, *a*). If the droplet charge exceeds critical value q_R (Rayleigh limit), droplets become unstable and produce a large number of daughter nanodroplets under the influence of Coulomb forces.

To formulate the requirements for plasma parameters at which fragmentation may occur, one needs to determine the value of critical droplet charge q_R in plasma. One way to estimate this value is to use the classical Rayleigh limit obtained for a charged droplet in vacuum [3]:

$$q_R = 4\pi\left((N+2)\varepsilon_0\sigma R_d^3\right)^{1/2}. \qquad (1)$$

Here, R_d is the droplet radius, ε_0 is the dielectric constant, σ is the surface tension coefficient, and $N \geqslant 2$ is the number of the mode entering an unstable state. Since the critical charge in this approximation increases with the mode number, the droplet stability may be analyzed by examining the transition to an unstable state of mode $N = 2$ only. The authors of [4] have analyzed the plasma parameters for droplets of different sizes at which criterion (1) is satisfied in the case of $N = 2$. However, further research revealed that the development of Rayleigh instability on the surface of submicron droplets in laser torch plasma has significant features that limit the applicability of criterion (1).

Let us illustrate this by examining in more detail the conditions for the development of electrocapillary instability on the surface of a droplet in plasma. It is known that when a metal droplet is charged in plasma (Fig. 1, *b*), a positively charged layer, which screens the droplet charge (Langmuir layer), forms. Langmuir layer thickness L_{sh} is several times larger than Debye radius of plasma $r_D = (\varepsilon_0 k_B T_e / q_e^2 n_{pl})^{1/2}$, where k_B is the Boltzmann constant, T_e is the plasma electron temperature, q_e is the electron charge, and n_{pl} is the plasma density. Note that the Debye radius for dense laser torch plasma assumes the values of $r_D \sim 10^{-8}$ m, which are significantly smaller than droplet radius $R_d \sim 10^{-7}$–10^{-6} m. Therefore, in the present study, we neglect the intrinsic curvature of the droplet surface and consider the condition for instability development in the planar approximation.

The transition of a charged metal droplet into an unstable state occurs when the negative pressure of the electric field overcomes the influence of capillary forces and the pressure of plasma ions at the peaks of the disturbed surface. Since Rayleigh limit (1) was obtained for a charged droplet in vacuum, it is applicable only if the influence of ion pressure may be neglected and the electric field lines are effectively focused at the peaks of the disturbed surface.

The distribution of electric field pressure $P_E = \varepsilon_0 E^2/2$ (E is the electric field strength) and plasma ion pressure $P_i = m_i n_i v_i^2/2$ (m_i is the ion mass, n_i is the ion density, and v_i is the ion velocity) along the droplet surface is governed by the charge distribution in the Langmuir layer and the value of floating potential U_{fl} of a droplet. In the planar case, the floating potential value is determined from relation $q_e U_{fl} = k_B T_e \ln(m_i/2\pi m_e)^{1/2}$, where m_e is the electron mass.

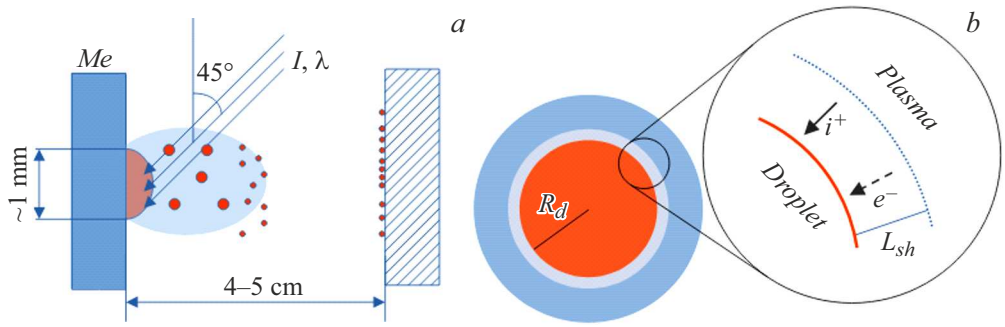


Figure 1. *a* — Diagram of the laser electrodispersion method. The incidence of laser radiation on the metal surface is accompanied by the ejection of droplets into plasma. Their charging in plasma leads to cascade electrodispersion and the formation of nanoparticles. The laser pulse parameters are as follows: power, 1–3 GW/cm^2; duration, 25 ns; radiation wavelength, 1064 nm. The pulse rate is 60 Hz. *b* — Langmuir layer forming around a droplet with radius R_d in laser torch plasma. The droplet charge is determined from the balance of currents of plasma ions i^+ and electrons e^-. At typical laser torch plasma parameters, layer thickness L_{sh} is significantly smaller than the droplet radius ($L_{sh} \ll R_d$).

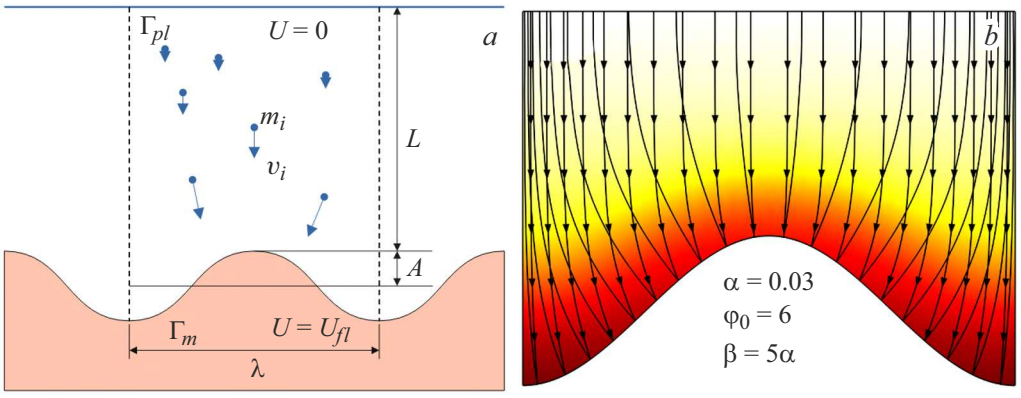


Figure 2. *a* — Diagram of computational region Ω. *b* — Example calculation of the Langmuir layer in the vicinity of a curved melt surface. The color gradient denotes the $n_i - n_e$ charge density. Darker regions correspond to higher charge densities. The curves with arrows are ion current lines, while the curves without arrows are electric field lines. A color version of the figure is provided in the online version of the paper.

The region of the Langmuir layer near the disturbed melt surface (Ω) is shown in Fig. 2, *a*. Cartesian xy-coordinates are used to characterize the geometry of this region. Disturbed metal surface Γ_m has the form of a plane wave: $y_m \sim A\cos(2\pi x/\lambda)$, where λ is the wavelength. The choice of this type of disturbance allows one to use this model to obtain a dispersion relation for waves on the melt surface. The characteristic width of the layer region is chosen in the calculation process in accordance with the surface charge screening condition (the electric field strength at tentative boundary Γ_{pl} between the layer and plasma should be significantly lower than the field strength at the surface of melt Γ_m).

In order to determine the field strength and the density and velocity of ions on the metal surface, one needs to solve the system of layer equations that consists of the continuity equation for the ion flux in the layer, the Newton equation for acceleration of ions under the influence of an electric field, and the Poisson equation for the distribution of electric field potential U in the layer. It is assumed below that the transport of ions in the layer is collisionless and the distribution of plasma electrons in the layer follows the Boltzmann distribution (Bohm approximation [5]). It is convenient to solve the problem in dimensionless quantities:

$$\xi = \frac{x}{\lambda},\ \eta = \frac{y}{\lambda},\ \rho = \frac{n_i}{n_{pl}},\ v = \frac{v_i}{c_i},\ \varphi = \frac{q_e U}{k_B T_e}, \qquad (2)$$

where $c_i = (k_B T_e/m_i)^{1/2}$ is the ion-sound velocity equal to the velocity of ions entering the layer (Bohm criterion). The system of layer equations has the following dimensionless form:

$$\mathrm{div}(\rho v) = 0, \qquad (3)$$

$$(v\nabla)v = \nabla\varphi, \qquad (4)$$

$$\alpha^2\Delta\varphi = \rho - e^{-\varphi}, \qquad (5)$$

where parameter $\alpha = r_D/\lambda$ characterizes the layer thickness relative to a given wavelength. Conditions $\rho = 1$, $v_\xi = 0$, $v_\eta = -1$, and $\varphi = 0$ are fulfilled at boundary Γ_{pl}. Since ion transport equations (3), (4) are first-order hyperbolic

ones and require boundary conditions on just one boundary to be defined, only the Dirichlet conditions for electric field potential equation (5) are specified on metal surface Γ_m: $\varphi = \varphi_0$, where $\varphi_0 = q_e U_{fl}/k_B T_e$ is the dimensionless floating potential. Periodic conditions are satisfied at vertical boundaries $\xi = \pm 1/2$. Since the floating potential depends logarithmically on the ion mass, it varies little when different metals are examined. The φ_0 value for metals used in applied research (Ni, Cu, Pt, Pd, etc.) falls within the range of 4–6. In the present study, φ_0 assumes a fixed value $\varphi_0 = 6$ in order to reduce the number of free parameters. The dimensionless amplitude of surface disturbance has the form $\beta = A/\lambda$ and assumes values $\beta = 0$–0.2. This range was chosen out of necessity of examining small disturbances of the droplet surface, which enables one to analyze the calculation results in a linear approximation.

The Bohm equations system was solved by the DG method [6] in Comsol Multiphysics. An example solution is illustrated in Fig. 2, *b*.

The calculation results revealed that the pressure of ions and the electric field is modulated along the surface at a small amplitude of surface disturbance; i.e., $P_{i,E} \approx P_{i0,E0} + \delta P_{i,E}\beta\cos(2\pi\xi)$, where $P_{i0,E0}$ is the pressure on a flat surface and $\delta P_{i,E}$ is the pressure modulation amplitude. The ion pressure on an undisturbed surface compensates completely for the electric field pressure; i.e., $P_{i0} = P_{E0}$. The amplitudes of modulation of electric field pressure δP_E, ion pressure δP_i, and total pressure $\delta P_{tot} = \delta P_E - \delta P_i$ normalized to thermal pressure of plasma $P_0 = n_{pl} k_B T_e$ corresponding to different values of parameter α are presented in Fig. 3.

It follows from the analysis of calculation data that both the ion pressure and the effect of limited focusing of electric field lines at the disturbance peaks, which is caused by the small thickness of the Langmuir layer, need to be taken into account at $\alpha < 1$ (long waves). Ion pressure is the most effective when the disturbance amplitude is greater than (or comparable to) the layer thickness. At $\alpha > 1$ (short waves), the ion pressure and the effect of limited focusing of field lines may be neglected. The amplitude of the electric field pressure modulation then approaches the vacuum case, enabling the use of classical Rayleigh limit (1) for qualitative assessments.

The restriction on the wavelength at which expression (1) is applicable leads to its modification. The wavelength on the droplet surface is determined based on mode number N of the natural droplet oscillation: $N\lambda = 2\pi R_d$. With the $\alpha \geqslant 1$ constraint taken into account, the lowest mode is $N \approx 2\pi R_d/r_D$. The expression for the Rayleigh limit for large droplets ($R_d \gg r_D$) in plasma then takes the form

$$q_R \approx 4\pi\left(\left(\frac{2\pi R_d}{r_D} + 2\right)\varepsilon_0\sigma R_d^3\right)^{1/2}$$

$$\approx 4\sqrt{2}\pi^{3/2} R_d\left(\frac{\varepsilon_0\sigma}{r_D}\right)^{1/2}. \qquad (6)$$

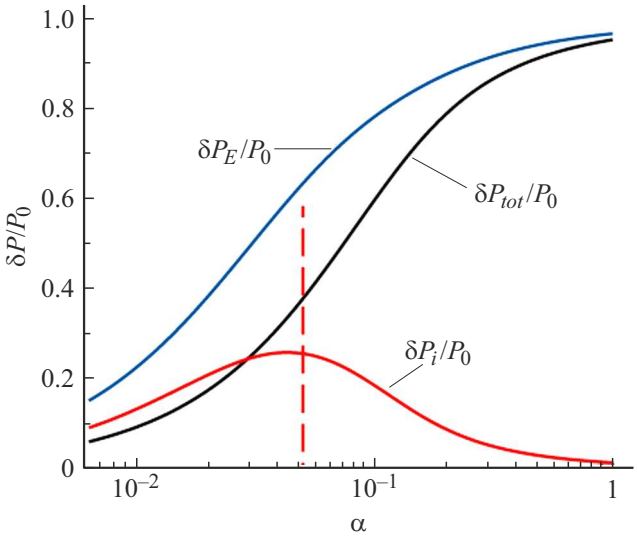


Figure 3. Plasma pressure modulation amplitude normalized to thermal pressure $P_0 = n_{pl} k_B T_e$. The vertical dashed line marks the value of α at which the amplitude reaches the layer thickness ($\beta = \alpha$).

It should be noted that condition (6) allows one to obtain the conditions for transition to an unstable state of high modes only. However, despite the fact that the efficiency of focusing of electric field lines is reduced in the long-wave region, the development of electrocapillary instability in this region is also possible [7]. The expression for the critical charge of a droplet valid within the entire wavelength range will be derived in future studies.

Funding

This study was carried out under the state assignment of the Ioffe Institute (project No. 0040-2019-0010).

Conflict of interest

The authors declare that they have no conflict of interest.

References

[1] V.M. Kozhevin, D.A. Yavsin, V.M. Kouznetsov, V.M. Busov, V.M. Mikushkin, S.Y. Nikonov, S.A. Gurevich, A. Kolobov, J. Vac. Sci. Technol. B, **18** 1402 (2000). DOI: 10.1116/1.591393

[2] S.M. Nevskaya, S.A. Nikolaev, Yu.G. Noskov, T.N. Rostovshchikova, V.V. Smirnov, S.A. Gurevich, M.A. Zabelin, V.M. Kozhevin, P.A. Tret'yakov, D.A. Yavsin, A.Yu. Vasil'kov, Kinet. Catal., **47**, 638 (2006). DOI: 10.1134/S0023158406040203.

[3] C.D. Hendricks, J.M. Schneider, Am. J. Phys., **31**, 450 (1963). DOI: 10.1119/1.1969579

[4] A.A. Bormatov, V.M. Kozhevin, S.A. Gurevich, Tech. Phys., **66** (5), 705 (2021). DOI: 10.1134/S1063784221050078.

[5] R.N. Franklin, J. Phys. D, **36**, R309 (2003). DOI: 10.1088/0022-3727/36/22/R01

[6] C.W. Shu, in *Building bridges: connections and challenges in modern approaches to numerical partial differential equations*. Ser. Lecture notes in computational science and engineering (Springer, Cham, 2016), vol. 114, p. 371–399. DOI: 10.1007/978-3-319-41640-3_12
[7] J.T. Holgate, M. Coppins, J.E. Allen, Appl. Phys. Lett., **112**, 024101 (2018). DOI: 10.1063/1.5013934

Translated by D.Safin